International Journal of Recent Technology and Engineering (IJRTE)
ISSN: 2277-3878 (Online), Volume-8 Issue-4, November 2019

Computational Experiment of Swirling Flows of Turbulence Models SA and SST.

Nazarov Farrukh Kholiyorovich, Khasanov Saidamin Magrupovich, Yakubov Asror Abduhalilovich

Abstract: ***The article numerically solves the problem of a swirling two-phase flow in a separator using the Menter model (SST) and Spalart-Allmaras (SA). The computational domain, which consists of coaxial cylinders and a conical part, is reduced to a rectangular shape by a change of coordinates. The stream function and vorticity of the flow are introduced, the first equation for which is solved by the upper relaxation method and the "upstream" scheme is used to solve the second of them. To describe the motion of solid particles with a low concentration, we use the Lograngе approach.The numerical results of applying both turbulence models are compared.***

Keywords: turbulent flow, SST model, SA model, implicit scheme, counter-flow scheme, Lagrangian approach, numerical solution.

I. INTRODUCTION

The intensive development of aviation, shipbuilding, and transport has attracted great attention to the study of separated flows at various values of operating parameters and configurations of streamlined bodies. Separate flow is a frequently occurring and, at the same time, most difficult to study type of motion of a real liquid [1]. The main feature of separated flows is that after the separation of the flow, the flow becomes unsteady [2,3,4]. Bearing capabilities of the wings, aerodynamic characteristics of aircraft, ships and submarines, the effectiveness of hydraulic machines and wind turbines are directly dependent on the development of flow separation. The origin and development of flow separation, the characteristics of separated flows are determined by a large number of parameters. The study of this complex phenomenon has been the subject of many experimental [3, 4, 5] and theoretical works [1, 6, 7].

Manuscript published on November 30, 2019.
* Correspondence Author
Nazarov Farrukh Kholiyorovich*, Graduate student, Institute of Mechanics and Seismic Resistance M.T. Urazbaeva Academy of Sciences of the Republic of Uzbekistan Fluid and gas mechanics,
farruxnazar@mail.ru.
Khasanov Saidamin Magrupovich, Head of the Department of "strength of Materials and Machine Details" Mechanical Faculty of Tashkent State Technical University,
xasanov1947@mail.com.
Yakubov Asror Abduhalilovich, Senior lecturer of the "strength of Materials and Machine Details" Department of Mechanics, Tashkent State Technical University Аннотация
asroryakubov@mail.ru.

The first theoretical results on flow separation were obtained using the classical theory of the boundary layer, which, however, does not allow one to take into account the strong interaction of the boundary layer with the external flow. The most important theoretical and practical results on the calculation of flows with flow separation were obtained using the asymptotic theory of a viscous fluid and semi-empirical methods based on an a priori choice of a flow model based on numerical or physical experiments [6].Among the various approaches applied to solving this problem, mathematical modeling based on the Navier-Stokes equations occupies an important place. At present, its role is increasing with the development of computer capabilities, the improvement of the models and numerical methods used, and also in connection with the possibility of replacing a costly, and in some cases practically impossible physical experiment. Complementing each other, calculation and experiment provide new opportunities for studying complex interdependent processes.

The main problem in obtaining non-stationary solutions of the Navier-Stokes equations of an incompressible fluid lies in the difficulties of simultaneously solving the equations of momentum and the continuity equation. At the first stage of the development of numerical algorithms for solving the Navier – Stokes equations for incompressible flows, variable vorticity and stream function were more often used [7, 8, 9]. Based on this approach, a large number of applied problems were solved, but the calculation of spatial problems using current functions is very difficult. The use of physical variables allows us to solve two-dimensional and three-dimensional problems according to a single algorithm. The main mathematical problems in solving the Navier-Stokes equations are associated with various types of differential equations for the laws of conservation of mass and quantity

Physical statement of the problem. The flow behavior in the dust collector is shown schematically in Fig. 1. As can be seen from the figure, the dust collector consists of concentric cylinders and cones.

Air is introduced in a tangential direction at the top of the dust collector body. Since the flow is limited by the cylindrical wall of the inner radius and the outer radius, an additional forced downward movement occurs. Next, the stream is divided into two parts. The main phase with a low density (inertia) is inverted and discharged through a pipe into an open atmosphere. Large particles accumulate around the wall and move down.

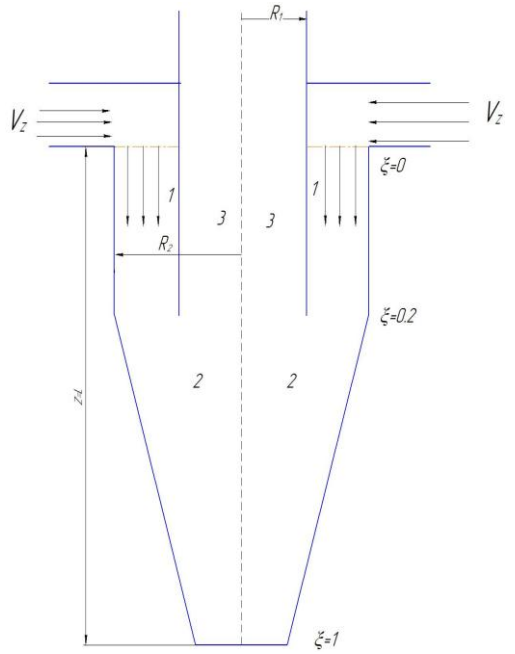

Fig. 1. Schematic diagram of a centrifugal dust collector

Mathematical statement of the problem.

The movements in a centrifugal dust collector are complex due to the multifactorial nature of the process in mathematical modeling. In contrast to [11], it is desirable to use the averaged Navier – Stokes equations. Because the flow has an axis of symmetry, then the equations are written in cylindrical coordinates:

$$\begin{cases} \frac{\partial V_z}{\partial z}+\frac{\partial r V_r}{r\partial r}=0, \\ \frac{\partial V_z}{\partial t}+V_r\frac{\partial V_z}{\partial r}+V_z\frac{\partial V_z}{\partial z}+\frac{1}{\rho}\frac{\partial P}{\partial z}=\frac{1}{r}\frac{\partial}{\partial r}\left[r(\nu+\nu_t)\frac{\partial V_z}{\partial r}\right], \\ \frac{\partial V_r}{\partial t}+V_r\frac{\partial V_r}{\partial r}+V_z\frac{\partial V_r}{\partial z}-\frac{V_\varphi^2}{r}+\frac{1}{\rho}\frac{\partial P}{\partial r}=\frac{1}{r}\frac{\partial}{\partial r}\left[r(\nu+\nu_t)\frac{\partial V_r}{\partial r}\right], \\ \frac{\partial V_\varphi}{\partial t}+V_r\frac{\partial V_\varphi}{\partial r}+V_z\frac{\partial V_\varphi}{\partial r}+\frac{V_\varphi V_r}{r}=\frac{1}{r}\frac{\partial}{\partial r}\left[r(\nu+\nu_t)\frac{\partial V_\varphi}{\partial r}\right]-\frac{\nu+\nu_t}{r^2}V_\varphi \end{cases} \quad (1)$$

In these systems, V_z, V_r, V_φ – respectively, axial, radial and tangential components of the airflow velocity vector; ν – is its molecular viscosity; ν_t – turbulent airflow viscosity; p – pressure.

On the walls, all components of the velocity vector are equal to zero;

for $z=0$ and $0<r<R_1$:

$V_r=V_r(r),\ V_z=V_z(r),\ V_\varphi=V_\varphi(r);$

for $z=0$ and $R_1<r<R_2$:

$V_r=V_\varphi=0,\ \frac{\partial V_z}{\partial r}=0;$

for $z=L$: $\frac{\partial^2 V_r}{\partial r^2}=0,\ \frac{\partial^2 V_z}{\partial r^2}=0,\ \frac{\partial^2 V_\varphi}{\partial r^2}=0.$

The initial conditions for the stream function were made by the iterative method of zero vorticity value. According to found speed V_r, V_z.

Modeling turbulence. To close the Reynolds-averaged Navier-Stokes equations, one-parameter differential models SA [12, 13] and SST [14], which are developed for external subsonic aerodynamics, are used.

The one-parameter Spalart-Allmaras (SA) turbulence model [12] was developed in 1992 and is intended to describe equilibrium flows such as a boundary layer for external flow problems at small angles of attack with small separation zones. Turbulence generation is determined by the rotor of the velocity field.

The SST model is a combination of k-ε and k-ω models, providing a combination of the best qualities of these long-known models. Thus, the k-ε model proved to be good in calculating free and jet shear flows, for the analysis of which its first version, proposed by Harlow, was actually intended, and the k-ω model provides a much more accurate description of the wall boundary layers.

To close equations (1), the turbulence models SST and SA are used.

The turbulence model SST have the form:

$$\begin{cases} \frac{\partial k}{\partial t}+V_z\frac{\partial k}{\partial z}+V_r\frac{\partial k}{\partial r}=\frac{\partial}{r\partial r}\left[(\mu+\sigma_k\mu_t)r\frac{\partial k}{\partial r}\right]+P-\beta^*\omega k, \\ \frac{\partial \omega}{\partial t}+V_z\frac{\partial \omega}{\partial z}+V_r\frac{\partial \omega}{\partial r}=\frac{\partial}{r\partial r}\left[(\mu+\sigma_\omega\mu_t)r\frac{\partial \omega}{\partial r}\right]+\frac{\gamma}{\nu_t}P-\beta\omega^2+2(1-F_1)\frac{\sigma_{\omega 2}}{\omega}\frac{\partial \omega}{\partial r}\frac{\partial k}{\partial r}. \end{cases} \quad (2)$$

SA model in cylindrical coordinates:

$$\frac{\partial \tilde{\nu}}{\partial t}+V_r\frac{\partial \tilde{\nu}}{\partial r}+V_z\frac{\partial \tilde{\nu}}{\partial z}=(P_w-D_w)+\frac{1}{\sigma}\left[\frac{1}{r}\frac{\partial}{\partial r}\left(r(\nu+\tilde{\nu})\frac{\partial \tilde{\nu}}{\partial r}\right)+C_{b2}\left(\frac{\partial \tilde{\nu}}{\partial r}\right)^2\right] \quad (3)$$

The turbulent viscosity is determined for the SST model from the ratio: $\nu_t=\frac{a_1 k}{(a_1\omega,\ \Omega F_2)}$, and for model SA: $\nu_t=\tilde{\nu}f_{v1}$.

II. SOLUTION METHOD

We include the ψ current function in the system according to the dependencies:

$$V_r=-\frac{1}{r}\frac{\partial \psi}{\partial \varphi},\quad V_z=\frac{1}{r}\frac{\partial \psi}{\partial r} \quad (4)$$

and vorticity

$$\zeta=\frac{\partial V_z}{\partial r}-\frac{\partial V_r}{\partial z}. \quad (5)$$

As a result, we come to a new system:

$$\begin{cases} \frac{\partial \zeta}{\partial t}+V_r\frac{\partial \zeta}{\partial r}+V_z\frac{\partial \zeta}{\partial z}-\frac{V_r\zeta}{r}+\frac{1}{r^3}\frac{\partial G^2}{\partial z}= \\ =-\frac{1}{r^2}\frac{\partial}{\partial r}(r(\nu+\nu_t)\zeta)+\frac{1}{r}\frac{\partial^2}{\partial r^2}(r(\nu+\nu_t)\zeta), \\ \frac{1}{r}\frac{\partial^2\psi}{\partial r^2}-\frac{1}{r^2}\frac{\partial \psi}{\partial r}+\frac{1}{r}\frac{\partial^2\psi}{\partial z^2}=\zeta, \\ \frac{\partial G}{\partial t}+V_r\frac{\partial G}{\partial r}+V_z\frac{\partial G}{\partial z}=\frac{\partial}{\partial r}\left[(\nu+\nu_t)\frac{\partial G}{\partial r}\right]-\frac{\nu+\nu_t}{r}\frac{\partial G}{\partial r}. \end{cases} \quad (6)$$

Here $G=\vartheta_\varphi r.$

If we denote $r^2=y$, system of equations (6) will be:

$$\begin{cases} \frac{\partial \zeta}{\partial t}+V_z\frac{\partial \zeta}{\partial z}+2\sqrt{y}V_r\frac{\partial \zeta}{\partial y}-\frac{V_r\zeta}{\sqrt{y}}+\frac{1}{\sqrt{y^3}}\frac{\partial G^2}{\partial z}= \\ =4\sqrt{y}\frac{\partial^2}{\partial y^2}\left(\sqrt{y}(\nu+\nu_t)\zeta\right), \\ 4y\frac{\partial^2\psi}{\partial y^2}+\frac{\partial^2\psi}{\partial z^2}=\zeta\sqrt{y}, \\ \frac{\partial G}{\partial t}+V_z\frac{\partial G}{\partial z}+2\sqrt{y}V_r\frac{\partial G}{\partial y}= \\ =2\sqrt{y}\frac{\partial}{\partial y}\left[2\sqrt{y}(\nu+\nu_t)\frac{\partial G}{\partial y}\right]-2(\nu+\nu_t)\frac{\partial G}{\partial y}. \end{cases} \quad (7)$$

To come to the regular calculation area, the coordinates were changed:

Retrieval Number: D7720118419/2019©BEIESP
DOI:10.35940/ijrte.D7720.118419
Journal Website: www.ijrte.org

Published By:
Blue Eyes Intelligence Engineering
& Sciences Publication

$$\xi = \frac{z}{L}, \quad \eta = \frac{y}{f(z)},$$

$$\begin{cases} f(z) = R \ \ npu \ \ z < 0, \\ f(z) = R - \dfrac{R-h}{L} z \ \ npu \ \ 0 < z < L. \end{cases}$$

Choosing these permutations in equations (7), we obtain the following result:

$$\begin{cases} \dfrac{\partial\zeta}{\partial t} + \dfrac{V_z}{L}\dfrac{\partial\zeta}{\partial\xi} + \left(\dfrac{2\sqrt{y}V_r}{f(z)} + V_z\eta'\right)\dfrac{\partial\zeta}{\partial\eta} - \dfrac{V_r\zeta}{\sqrt{y}} + \dfrac{1}{\sqrt{y^3}L}\dfrac{\partial G^2}{\partial\xi} + \dfrac{\eta'}{\sqrt{y^3}}\dfrac{\partial G^2}{\partial\eta} = \\ = \dfrac{4\sqrt{y}}{f^2(z)}\dfrac{\partial^2}{\partial\eta^2}\left(\sqrt{y}(\nu+\nu_t)\zeta\right), \\ \dfrac{1}{L^2}\dfrac{\partial^2\psi}{\partial\xi^2} + \eta''\dfrac{\partial\psi}{\partial\eta} + \dfrac{2\eta'}{L}\dfrac{\partial^2\psi}{\partial\xi\partial\eta} + \left(\dfrac{4y}{f^2(z)} + (\eta')^2\right)\dfrac{\partial^2\psi}{\partial\eta^2} = \zeta\sqrt{y}, \\ \dfrac{\partial G}{\partial t} + \dfrac{V_z}{L}\dfrac{\partial G}{\partial\xi} + \left(\dfrac{2\sqrt{y}V_r}{f(z)} + V_z\eta'\right)\dfrac{\partial G}{\partial\eta} = \\ = \dfrac{2\sqrt{y}}{f(z)}\dfrac{\partial}{\partial\eta}\left[\dfrac{2\sqrt{y}(\nu+\nu_t)}{f(z)}\dfrac{\partial G}{\partial\eta}\right] - \dfrac{2(\nu+\nu_t)}{f(z)}\dfrac{\partial G}{\partial\eta}. \end{cases} \tag{8}$$

Substituting these substitutions and marking (2) and (3), we obtain the following results:

$$\begin{cases} \dfrac{\partial k}{\partial t} + \dfrac{V_z}{L}\dfrac{\partial k}{\partial\xi} + \left(\dfrac{2\sqrt{y}V_r}{f(z)} + V_z\eta'\right)\dfrac{\partial k}{\partial\eta} = \\ = \dfrac{2}{f(z)}\dfrac{\partial}{\partial\eta}\left[\dfrac{2y(\mu+\sigma_k\mu_t)}{f(z)}\dfrac{\partial k}{\partial\eta}\right] + P - \beta^*\omega k, \\ \dfrac{\partial\omega}{\partial t} + \dfrac{V_z}{L}\dfrac{\partial\omega}{\partial\xi} + \left(\dfrac{2\sqrt{y}V_r}{f(z)} + V_z\eta'\right)\dfrac{\partial\omega}{\partial\eta} = \dfrac{2}{f(z)}\dfrac{\partial}{\partial\eta}\left[\dfrac{2y(\mu+\sigma_\omega\mu_t)}{f(z)}\dfrac{\partial\omega}{\partial\eta}\right] + \\ + \dfrac{\gamma}{\nu_t}P - \beta\omega^2 + 8y(1-F_1)\dfrac{\sigma_{\omega 2}}{f^2(z)\omega}\dfrac{\partial\omega}{\partial\eta}\dfrac{\partial k}{\partial\eta}. \end{cases} \tag{9}$$

$$\frac{\partial\tilde{\nu}}{\partial t} + \frac{V_z}{L}\frac{\partial\tilde{\nu}}{\partial\xi} + \left(\frac{2\sqrt{y}V_r}{f(z)} + V_z\eta'\right)\frac{\partial\tilde{\nu}}{\partial\eta} = (P_w - D_w) + \tag{10}$$

$$+ \frac{1}{\sigma}\left[2\frac{\partial}{\partial\eta}\left(\frac{2y(\nu+\tilde{\nu})}{f(z)}\frac{\partial\tilde{\nu}}{\partial\eta}\right) + 4yC_{б2}\left(\frac{\partial\tilde{\nu}}{f(z)\partial\eta}\right)^2\right]$$

Border conditions. On the wall, all speeds will be zero, and on wasps $\frac{\partial F}{\partial y} = 0$ for F=V_z, ν, k, ω and G; V_r=0. To start the calculation, the values were set $\tilde{\nu} = 3/\mathrm{Re}$, $k_{in} = \frac{3}{2}(V_z I)^2$, $\omega_{in} = \frac{k^{1/2}}{C_\mu^{1/4} l}$ at *Re=10000.*

To ensure the stability of the computational process in the approximation of convective terms, a difference scheme was used against the flow of A.A. The Poisson equation for the stream function was also approximated by the central difference and the iteration method with upper relaxation was used to resolve it [15].

After changing the coordinate of equation (8), the following form changes:

$$\begin{cases} \dfrac{\zeta_{i,j}^{n+1} - \zeta_{i,j}^n}{\Delta t} + 0.5(UU + |UU|)\dfrac{\zeta_{i,j}^n - \zeta_{i-1,j}^n}{\Delta\xi} + 0.5(UU - |UU|)\dfrac{\zeta_{i+1,j}^n - \zeta_{i,j}^n}{\Delta\xi} + \\ + 0.5(VV + |VV|)\dfrac{\zeta_{i,j}^n - \zeta_{i,j-1}^n}{\Delta\eta} + 0.5(VV - |VV|)\dfrac{\zeta_{i,j+1}^n - \zeta_{i,j}^n}{\Delta\eta} - \dfrac{V_{r,i,j}\zeta_{i,j}^n}{\sqrt{y}} + \\ + \dfrac{\zeta_{i,j}^n\psi_{i,j}^n - \zeta_{i-1,j}^n\psi_{i-1,j}^n}{\sqrt{y^3}L\Delta\xi} + \eta'\dfrac{\zeta_{i,j}^n\psi_{i,j}^n - \zeta_{i,j-1}^n\psi_{i,j-1}^n}{\sqrt{y^3}\Delta\eta} = 4\sqrt{y}\dfrac{\left(\dfrac{\partial N}{\partial\eta}\right)_{i,j+0.5} - \left(\dfrac{\partial N}{\partial\eta}\right)_{i,j-0.5}}{\Delta\eta} \\ \dfrac{G_{i,j}^{n+1} - G_{i,j}^n}{\Delta t} + 0.5(UU + |UU|)\dfrac{G_{i,j}^n - G_{i-1,j}^n}{\Delta\xi} + 0.5(UU - |UU|)\dfrac{G_{i+1,j}^n - G_{i,j}^n}{\Delta\xi} + \\ + 0.5(VV + |VV|)\dfrac{G_{i,j}^n - G_{i,j-1}^n}{\Delta\eta} + \\ + 0.5(VV - |VV|)\dfrac{G_{i,j+1}^n - G_{i,j}^n}{\Delta\eta} = -\dfrac{(\nu+\nu_t)\left(G_{i,j+1}^n - G_{i,j-1}^n\right)}{f(z)\Delta\eta} \\ = \sqrt{y}\dfrac{(M_{i,j+1} + M_{ij})G_{i,j+1}^n - (M_{i,j+1} + 2M_{i,j} + M_{i,j-1})G_{i,j}^n + (M_{i,j} + M_{i,j-1})G_{i,j-1}^n}{f(z)\Delta\eta^2} \\ \dfrac{\psi_{i+1,j}^k - 2\psi_{i,j}^{k+1} + \psi_{i-1,j}^k}{(L\Delta\xi)^2} + \eta''\dfrac{\psi_{i,j+1}^k - \psi_{i,j-1}^k}{2\Delta\eta} + 2\eta'\dfrac{\psi_{i+1,j+1}^k - \psi_{i-1,j+1}^k + \psi_{i+1,j-1}^k - \psi_{i-1,j-1}^k}{L\Delta\xi\Delta\eta} + \\ + \left(\dfrac{4y}{f^2(z)} + (\eta')^2\right)\dfrac{\psi_{i,j+1}^k - 2\psi_{i,j}^{k+1} + \psi_{i,j-1}^k}{\Delta\eta^2} = \zeta_{i,j}^k\sqrt{y}. \end{cases} \tag{11}$$

Here $M_{i,j} = \dfrac{2\sqrt{y}(\nu+\nu_t)}{f(z)}$, $N = \sqrt{y_j}(\nu + \nu_{t,i,j})\zeta$.

To determine the turbulent viscosity on the system, equation (11) separately solved two turbulence models and compared the numerical results.

III. RESULTS

The parameters of the laboratory installation of the dust collector had the following values: $R_1 = 12 \ sm$, $R_2 = 20 \ sm$, $h = 12 \ sm$, $L = 300 \ sm$. The experiments were carried out with the following values of the flow parameters at the entrance to the coaxial channel: $V_z = 4.1 \ м/с$, $V_r = 0$, $V_\varphi = \frac{1.8}{r}\frac{м^2}{c}$.

In fig. 2 - 4 illustrate air velocity profiles in the cross section $\xi = 0.5$.

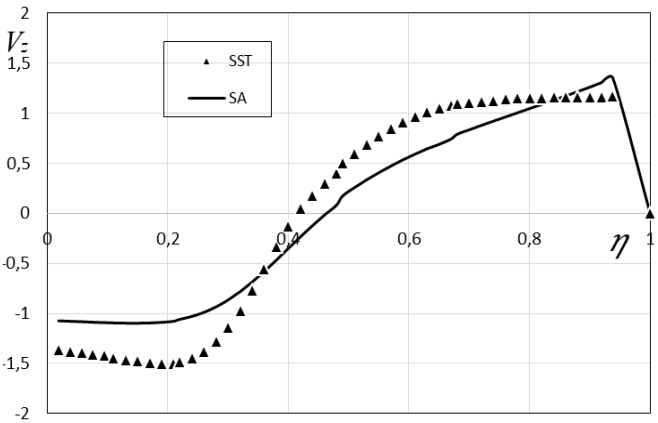

Fig. 2. The profiles of the axial velocity of the air flow in the section $\xi = 0.5$

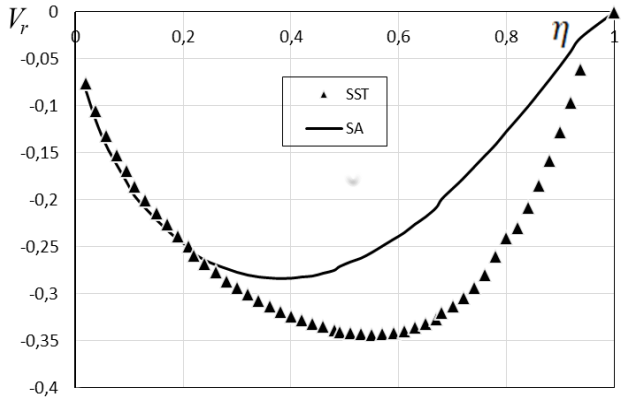

Fig. 3. The profiles of the radial air velocity in the cross section $\xi = 0.5$

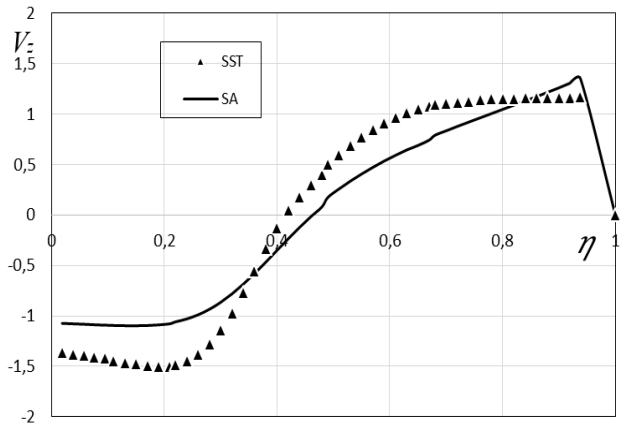

Fig. 3. The profiles of the radial air velocity in the cross section $\xi = 0.5$

We pass to the second stage. There are two approaches to modeling the motion of the solid phase (dust): Euler and Lagrange [10]. Euler's approach has the potential to account for double events. In the Lagrangian approach, we can trace the trajectory of the solid phase. For us, dust trajectories are important. Therefore, the Lagrangian approach was used in this study. As a result, the equations of motion of a solid particle (dust particle) have the following form [10]:

$$\begin{cases} \frac{\partial \vartheta_{iz}}{\partial t} + \vartheta_{ir}\frac{\partial \vartheta_{iz}}{\partial r} + \vartheta_{iz}\frac{\partial \vartheta_{iz}}{\partial r} = k_i(V_z - \vartheta_{iz}), \\ \frac{\partial \vartheta_{ir}}{\partial t} + \vartheta_{ir}\frac{\partial \vartheta_{ir}}{\partial r} + \vartheta_{iz}\frac{\partial \vartheta_{ir}}{\partial r} - \frac{\upsilon_{i\varphi}^2}{r} = k_i(V_r - \vartheta_{ir}), \\ \frac{\partial \vartheta_{i\varphi}}{\partial t} + \vartheta_{ir}\frac{\partial \vartheta_{i\varphi}}{\partial r} + \vartheta_{iz}\frac{\partial \vartheta_{i\varphi}}{\partial r} + \frac{\vartheta_{i\varphi}\vartheta_{ir}}{r} = k_i(V_\varphi - \vartheta_{i\varphi}) \end{cases} \quad (8)$$

Here V_r and V_φ air speed in directions r and φ, ϑ_{pr} и $\vartheta_{p\varphi}$ dust speed in directions r and φ, k — is the coefficient of interaction of air and particles. In these equations we get the pressure depending on the speed of the pipe u_0, sizes R_1, R_2 and dynamic pressure $\rho \cdot u_0^2$. We are using the interaction coefficient using the Stokes law: $k = \frac{18\mu R_1}{\rho d^2 u_0}$.

We use the Lagrange method to describe the motion of particles when the system of equations (8) [10] is washed down in the form:

$$\begin{cases} \frac{d\vartheta_{ir}}{dt} = \frac{\vartheta_{i\varphi}^2}{r} + k_i(V_r - \vartheta_{ir}) \\ \frac{d\vartheta_{iz}}{dt} = k_i(V_z - \vartheta_{iz}) \\ \frac{d\vartheta_{i\varphi}}{dt} = -\frac{\vartheta_{i\varphi}\vartheta_{ir}}{r} + k_i(V_\varphi - \vartheta_{i\varphi}) \end{cases} \quad (9)$$

Given the known values of V_z, V_r and V_φ, this system is solved by Euler numerical methods with a second order of accuracy.

In fig. Figures 5-6 show the trajectories of dust particles with diameters of $\delta = 7$ *мкм*, $\delta = 10$ *мкм* and $\delta = 13$ *мкм* that were obtained by the Spalart-Almaras method.

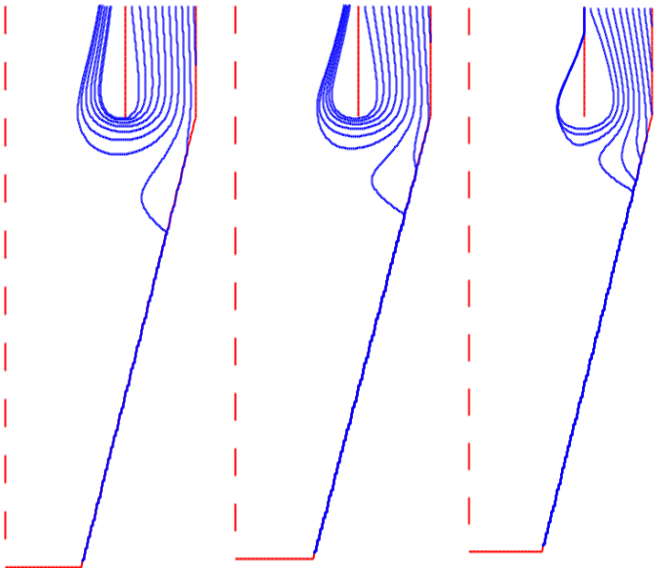

а) **б)** **в)**

Fig. 5. Particle trajectories obtained by SA models

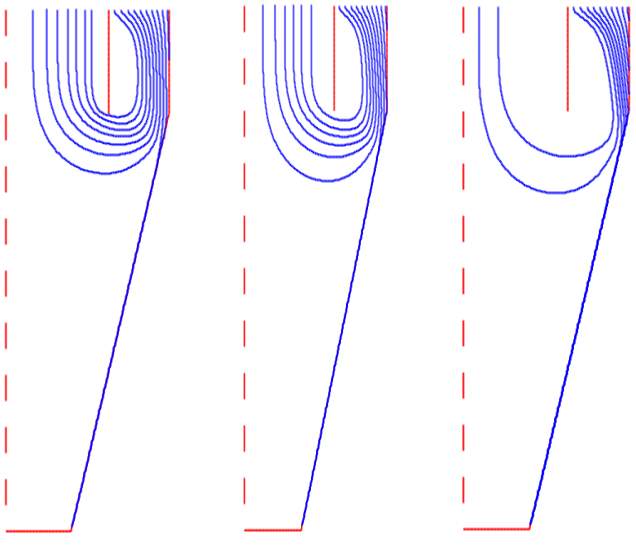

а) **б)** **в)**

***Fig. 6.* Particle trajectories obtained using the SST model.**

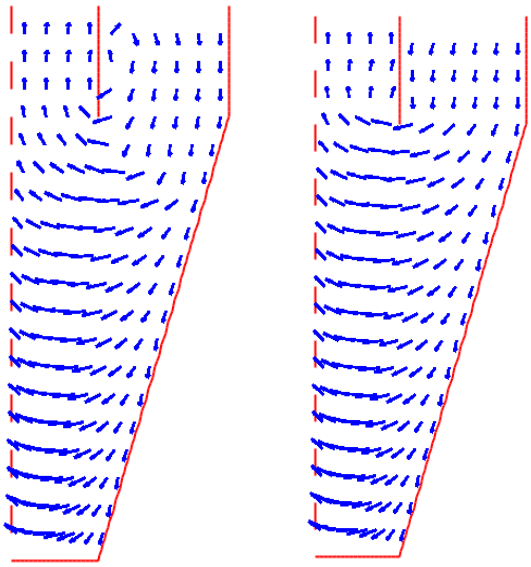

а) **б)**

Fig. 7. Vector velocity field in the central part: a) SST, b) SA

IV. FINDINGS

For the numerical simulation of unsteady turbulent separated incompressible flows, the Navier-Stokes equations averaged by Reynolds are used. The closure of the system of equations is carried out using the Menter MST turbulence model SST and Spalart-Allmaras (SA). Implementation of the approach used is performed using the developed software and methodological support for the numerical solution of the Navier-Stokes equations of an incompressible fluid in arbitrary orthogonal coordinates. Figure 5-6 shows that when a) the diameter with $\delta = 7\ mkm$ is approximately 30%, 30% and b) in diameter $\delta = 10\ mkm$, 40%, 40%, they are collected by a dust collector, that is, into the hopper. When the diameter $\delta = 13 mkm$ c) dust particles 70%, 80% fall into the hopper. As can be seen from the figures above, the numerical results of the SA and SST models are very close to each other.

REFERENCES

1. Gogish L.V. Turbulent Tear Currents/L.W.Gogish, G.U.Stepanov. - M.: Science, 1979. - 368s.
2. Belocerkovsky S.M., V.N.Kotovsky, M.I.Nist. Mathematical modeling of plane-parallel flow of bodies-M.: Science, 1988. - 232c.
3. Zhen P. Flow Off Control. Economy, Efficiency, Security/P.H. - Moscow: Mir, 1979. - 552 p.
4. Zhen P. Passage Currents/Zhen P. - M.: Mir, T.1, 1972 - 300c.; T.2, 1973. - 280 pages; T.3.1973. – 334 pages.
5. Paraschivoiu I. Wind turbine design with emphasis on Darrieus concept / I.Paraschivoiu. – Canada: Polytechnic international press, 2002. – 438p.
6. Gogish A.V., Neyland V.J., Stepanov G.Y. Theory of Two-Dimensional Tear Currents//Results of Science and Technology. Hydromechanical. - Moscow: Science, 1975. -8. - C.5-73.
7. Schlichting G. Boundary Layer Theory/G. Schlichting. - M.: Science, 1974. - 711c.
8. Roach P. Computational hydrodynamics/P.Pouch. - M.: Mir, 1980.-616s.
9. Gosmen A.M. Numerical methods of research of viscous fluid currents/A.M.Gosmen, Ban V.M., Ranchel A.K. et al. - M.: Mir, 1972. - 323s.
10. Baranov D.A., Kutepov A.M., Lagutkin M.G. Calculation of separation processes in hydro-cyclones // Theoretical foundations of chemical technology. - 1996. - V. 30. - No. 2. - Pp. 117–122.
11. Loytsyanskiy L. G. Mechanics of Liquid and Gas. - Moscow: Science, 1987.-678 p.
12. Spalart P.R., Allmaras S.R. A one-equation turbulence model for aerodynamic flow // AIAA Paper. – 1992.– 12;1. – P.439–478.
13. Shur M.L, Strelets M. K., Travin A.K., Spalart P.R. Turbulence modeling in rotating and curved channels: Assessing the Spalart-Shur correction //AIAA Journal. – 2000. – 38;5. – P.784–792.
14. Mentor, FR, "Turbulence Models with Two Equations for Engineering Applications," AIAA Journal, Vol. 32, No. 8, August 1994, pp. 1598-1605.
15. Samarsky A.A. Theory of difference schemes. Publishing House "Nauka", Moscow, 1977.

AUTHORS PROFILE

Research Interests Mathematical models of turbulent flows, numerical methods, multiphase flows. Scientific direction Fluid and gas mechanics Post graduate student

Scientific direction: Technology and processes of mechanical and physical, technical processing. Machine tools and equipment.

Scientific direction: Technology and processes of mechanical and physical, technical processing. Machine tools and equipment.